Myocardial Delivery of Lipidoid Nanoparticle Carrying modRNA Induces Rapid and Transient Expression

Irene C Turnbull[1], Ahmed A Eltoukhy[2], Kenneth M Fish[1], Mathieu Nonnenmacher[1], Kiyotake Ishikawa[1], Jiqiu Chen[1], Roger J Hajjar[1], Daniel G Anderson[2] and Kevin D Costa[1]

[1]Cardiovascular Research Center, Icahn School of Medicine at Mount Sinai, New York, New York, USA; [2]David H Koch Institute for Integrative Cancer Research, Massachusetts Institute of Technology, Cambridge, Massachusetts, USA

Nanoparticle-based delivery of nucleotides offers an alternative to viral vectors for gene therapy. We report highly efficient *in vivo* delivery of modified mRNA (modRNA) to rat and pig myocardium using formulated lipidoid nanoparticles (FLNP). Direct myocardial injection of FLNP containing 1–10 µg eGFPmodRNA in the rat (n = 3 per group) showed dose-dependent enhanced green fluorescent protein (eGFP) mRNA levels in heart tissue 20 hours after injection, over 60-fold higher than for naked modRNA. Off-target expression, including lung, liver, and spleen, was <10% of that in heart. Expression kinetics after injecting 5 µg FLNP/eGFPmodRNA showed robust expression at 6 hours that reduced by half at 48 hours and was barely detectable at 2 weeks. Intracoronary administration of 10 µg FLNP/eGFPmodRNA also proved successful, although cardiac expression of eGFP mRNA at 20 hours was lower than direct injection, and off-target expression was correspondingly higher. Findings were confirmed in a pilot study in pigs using direct myocardial injection as well as percutaneous intracoronary delivery, in healthy and myocardial infarction models, achieving expression throughout the ventricular wall. Fluorescence microscopy revealed GFP-positive cardiomyocytes in treated hearts. This nanoparticle-enabled approach for highly efficient, rapid and short-term mRNA expression in the heart offers new opportunities to optimize gene therapies for enhancing cardiac function and regeneration.

Received 3 April 2015; accepted 7 September 2015; advance online publication 1 December 2015. doi:10.1038/mt.2015.193

INTRODUCTION

The persistence of cardiovascular disease as a leading cause of death in the modern world motivates the development of novel treatments to regenerate cardiac tissue after injury and to restore lost function due to genetic and acquired diseases. Gene therapy offers one promising approach to solve this urgent human health need. For example, virus-based gene therapy using SERCA2a has shown promise for the treatment of heart failure in preclinical animal models and early clinical trials,[1,2] though it remains uncertain whether sufficient amounts of DNA can be delivered to produce clinically meaningful improvements in cardiac performance.[3] Also, overexpression of stem cell factor using injected adenovirus induces postinfarction cardiac repair and improves hemodynamic function in rats and pigs.[4,5] Nevertheless, viral delivery of DNA has limitations depending on the type of vectors used. Plasmid injections are inefficient and cause inflammation. Recombinant adenoviruses effectively transduce the myocardium but result in a significant inflammatory response, while adeno-associated vectors require 1 month for achieving peak expression.[6] Thus, for some biotherapeutic and basic science applications, it would be advantageous to rely on nonviral vectors that allow an efficient and controllable time course of gene expression after delivery.

Options for nonviral gene delivery have been made possible through advances in the field of nanomedicine, whereby a diversity of nanoparticles has been developed to deliver therapeutic agents for a range of biomedical applications.[7] To accelerate the nanoparticle design optimization process, the Anderson laboratory has pioneered the use of combinatorial chemistry approaches for high-throughput *in vitro* screening of classes of nanoparticle formulations,[8,9] demonstrating significant improvements in performance compared to alternative transfection reagents such as Lipofectamine. The resulting Stemfect RNA Transfection Reagent (commercially available through Stemgent, Cambridge, MA) is superior for *in vitro* and *in vivo* delivery of mRNAs compared to naked nucleotides for some applications.[10] Unique characteristics that make lipid-based nanoparticle formulations attractive for the delivery of mRNA include enhancement of cellular uptake and endosomal escape, protection of the conjugated mRNA from nuclease degradation, and compatibility with molecular surface modification using specific ligand receptors for targeted delivery. However, these nanoparticles have undergone limited testing *in vivo*, and have never specifically been assessed for cardiac delivery applications.

To achieve well-controlled expression kinetics, mRNA offers the advantage of inducing rapid protein expression within hours,[10] and subsequent degradation within days, as it only involves transport to the cytosol rather than incorporation into nuclear chromatin. But natural mRNA also has immunogenic potential.[11]

Correspondence: Kevin D Costa, Cardiovascular Cell and Tissue Engineering Laboratory, Cardiovascular Research Center, Icahn School of Medicine at Mount Sinai, One Gustave L. Levy Place, Box 1030, New York, New York 10029, USA. E-mail: kevin.costa@mssm.edu

Synthetic modification of mRNA nucleosides, such as replacing uridine with pseudouridine, has been shown to improve immunogenicity by diminishing activation of RNA-dependent protein kinase.[12] Carrier agents such as Lipofectamine can improve stability of modified mRNA (modRNA), but efficient delivery to nonendocytotic and nonproliferative cells, such as cardiomyocytes, remains challenging.[13,14] Due to the high cost of synthetic modRNA, clinical translation as a practical therapeutic option will require stability for off-the-shelf usage, efficient delivery to myocardium, and robust expression of desired proteins.

Toward this goal, the present study sought to develop a nanoparticle system for mRNA delivery that could improve upon currently available methods for gene therapy in cardiovascular disease by: (i) providing a nonviral gene transfer carrier, (ii) using a delivered agent with rapid and transient expression, and (iii) offering the highest possible cardiac efficiency. Such a nanoparticle-based system could enable alternative gene therapy approaches in cardiac regenerative nanomedicine, such as short-term delivery of cardio-regenerative factors to stimulate postinfarction repair while avoiding uncontrolled long-term growth or tumorigenesis.

RESULTS

As described below, we have developed a nanotechnology-based method of mRNA delivery for rapid and transient expression in the heart. An epoxide-derived lipidoid complex designated as C14-113[8] was combined with pseudouridine-modified modRNA encoding the fluorescent reporter eGFP to create formulated lipidoid nanoparticles (FLNP). These FLNP/eGFPmodRNA nanoparticles are shown here to be stable in storage at 4 °C for at least 2 weeks, and are efficient and effective for transducing myocardium in rats and pigs, either by direct intramyocardial injection or by intracoronary delivery.

Nanoparticle formulation stability

As shown in **Figure 1**, FLNP/eGFPmodRNA nanoparticle size (~155 nm diameter) was essentially constant for at least 15 days of storage in phosphate-buffered saline (PBS) solution at 4 °C. Also, although freshly synthesized particles were approximately twice as effective at transfecting cultured HeLa cells compared to stored particles, possibly reflecting an initial loss of functional particles due to, *e.g.*, particle adsorption, the transfection activity of stored particles was essentially independent of storage time from 1 to 15 days. Thus, the lipidoid nanoparticle formulation remains stable for at least 2 weeks in cold storage, allowing FLNP/modRNA nanoparticles to be conveniently prepared in advance of the therapeutic procedure for use when needed.

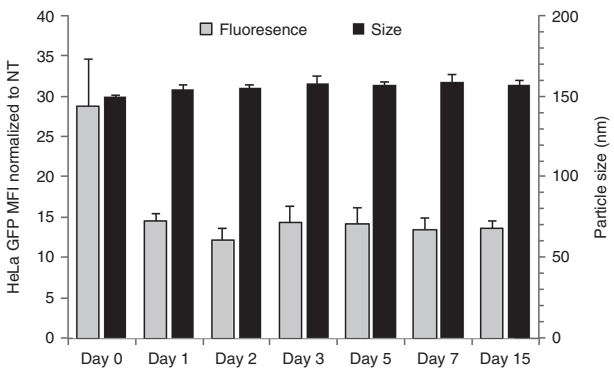

Figure 1 Stability of formulated lipidoid nanoparticles tested *in vitro* on the day of synthesis (day 0) and up to 15 days in storage at 4 °C. Geometric mean fluorescence intensity for cultured HeLa cells was measured 24 hours after transfection with 40 ng eGFPmodRNA (gray), relative to nontreated cells (mean ± SD, $n = 3$). Particle size (z-average diameter) was determined by dynamic light scattering (black) (mean ± SD, $n = 3$).

FLNP efficiently transfer mRNA to the heart *in vivo*

We examined the C14-113 lipidoid nanoparticle formulation[8] for the delivery of eGFPmodRNA to adult male rats via direct intramyocardial injection. As illustrated schematically in **Supplementary Figure S1a**, three different dosages of modRNA in freshly prepared nanoparticles were used and compared to saline-treated negative controls. Using quantitative real-time polymerase chain reaction (PCR) to measure eGFP mRNA levels relative to glyceraldehyde-3-phosphate dehydrogenase (GAPDH), the mRNA levels increased with dosage from 0.05 ± 0.04 at 1 µg to 1.97 ± 0.45 at 5 µg and 1.92 ± 1.09 at 10 µg compared to saline control (0.0004 ± 0.0001; $n = 3$ rats per group) evaluated 20 hours after injection (**Figure 2**, top panel). Note that GAPDH mRNA levels per microgram of RNA in the reverse-transcriptase reaction were consistent among conditions tested (**Supplementary Figure S2a**), so the eGFP/GAPDH ratios accurately reflect differences in eGFP mRNA. At a dose of approximately 0.02 mg/kg body weight, these results represent the highest efficiency to date for mRNA delivery to myocardium (compared to an estimated 0.66 and 3.3 mg/kg in the recent studies by Huang *et al.* and Zangi *et al.*, respectively[14,15]). We also investigated the efficacy of myocardial transduction using naked eGFPmodRNA at a dose of 10 µg in saline buffer, and found very low levels of eGFPmodRNA expression (0.031 ± 0.016) ($P = 1.0$ versus saline). Thus, at a matched modRNA dose of 10 µg, the use of FLNP nanoparticles significantly increased the efficiency of eGFPmodRNA delivery to the myocardium by more than 60-times compared to injection of naked modRNA ($P = 0.02$).

Myocardial delivery was further confirmed by immunofluorescent detection of GFP protein in frozen heart tissue sections (**Figure 2**, bottom panel). Hearts that received higher doses (5 and 10 µg) of FLNP/eGFPmodRNA showed robust presence of GFP-positive cells, while much lower expression was observed in the 1-µg FLNP/eGFPmodRNA and naked eGFPmodRNA-treated hearts. In all cases, the GFP-positive cells were concentrated in the subepicardial areas of injection, but their distribution also extended into the myocardium.

Transient expression achieved after intramyocardial injection of FLNP/modRNA

Assessment of expression kinetics was performed using direct intramyocardial injection of FLNP/eGFPmodRNA nanoparticles at the 5-µg dosage (**Supplementary Figure S1b**). PCR analysis revealed high levels of eGFP mRNA in the heart as early as 6 hours postdelivery (4.76 ± 1.9, $n = 5$), which decreased to approximately half this level at 48 hours (2.14 ± 1.13, $n = 5$), and was barely detectable at 14 days postdelivery (0.019 ± 0.009, $n = 3$). The data revealed a nearly exponential decay of eGFP mRNA level over the 2-week period (**Figure 3a**), with no systematic trends in GAPDH (**Supplementary Figure S2b**).

The time course of myocardial delivery was also confirmed by immunofluorescence. GFP-positive cells were observed in histological sections of heart tissue harvested at 6, 20, and 48 hours after FLNP/eGFPmodRNA nanoparticle injection (**Figure 3b**), in agreement with the PCR data that showed robust eGFP mRNA levels at these time points. No GFP-positive cells were identified in samples obtained at 60 hours and beyond. These data demonstrate a well-defined window of rapid and transient protein expression following FLNP/modRNA transfer to the heart.

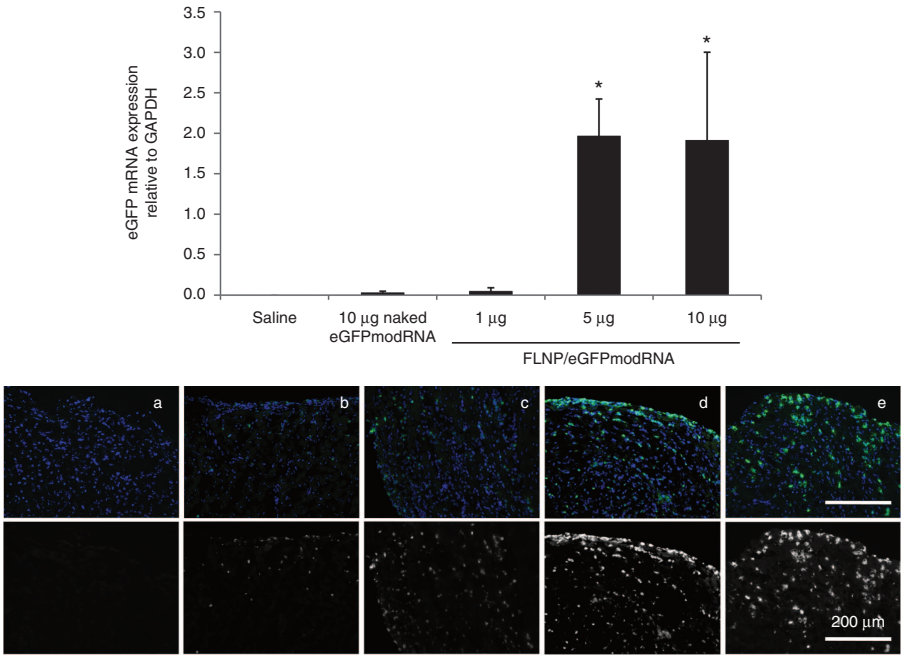

Figure 2 Dose response of intramyocardial injection of formulated lipidoid nanoparticles (FLNP)/eGFPmodRNA in rats. Top panel: Expression of eGFP mRNA measured by real-time polymerase chain reaction in rat myocardium 20 hours after intramyocardial injection of: FLNP with 1, 5, or 10 µg of eGFPmodRNA, and either saline or 10 µg of naked eGFPmodRNA as controls. Values represent mean (±SD) eGFP mRNA expression levels relative to GAPDH, $n = 3$ rats per group. *$P \leq 0.02$ versus naked eGFPmodRNA. Bottom panel: Immunofluorescence micrographs of corresponding frozen tissue sections of rat myocardium for (**a**) saline-only, (**b**) 10 µg naked eGFPmodRNA, and (**c–e**) FLNP/eGFPmodRNA at 1-µg (**c**), 5-µg (**d**), or 10-µg (**e**) doses. Sections incubated with anti-GFP antibody (green), and nuclei stained with DAPI (blue). Upper row shows pseudo-colored images with merged green and blue channels. Lower row shows only the green channel in grayscale. Scale bar = 200 µm for all panels. DAPI, 4',6-diamidino-2-phenylindole.

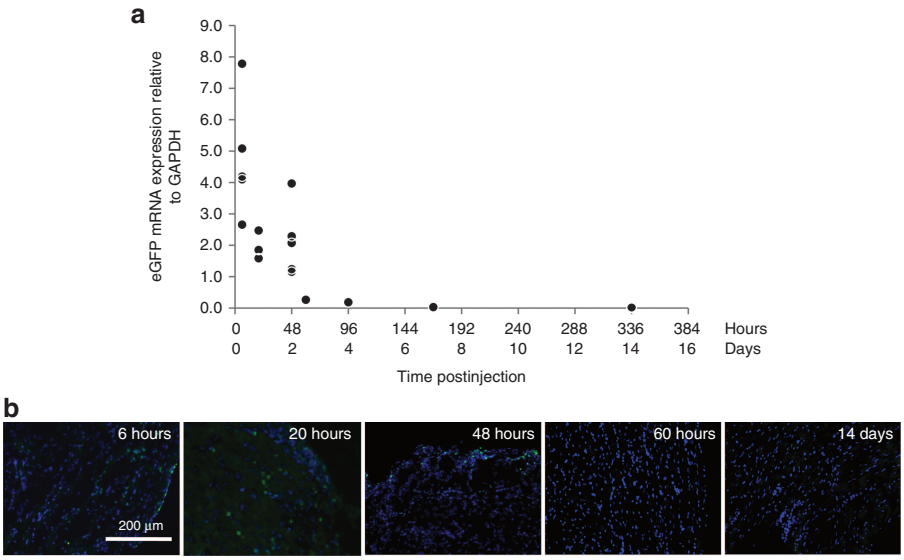

Figure 3 Expression kinetics after intramyocardial injection of FLNP/eGFPmodRNA in rats. (**a**) Expression of eGFP mRNA in rat myocardium measured by real-time polymerase chain reaction, from 6 hours to 14 days after intramyocardial injection of formulated lipidoid nanoparticles (FLNP) with 5 µg of eGFPmodRNA ($n = 1–5$ rats per time point, 19 total). Values represent eGFP mRNA expression levels relative to GAPDH, revealing a nearly exponential decay in mRNA with time postinjection. (**b**) Representative immunofluorescence microphotographs of frozen tissue sections of rat myocardium collected at selected time points (6 hours to 14 days) from the above study. Sections incubated with anti-GFP antibody (green), and nuclei stained with DAPI (blue). Scale bar = 200 µm for all panels. DAPI, 4',6-diamidino-2-phenylindole.

Biodistribution analysis shows minimal off-target modRNA expression

To assess off-target delivery and expression, several organs were sampled along with the heart 20 hours after direct intramyocardial injection of FLNP/eGFPmodRNA (5 μg), including lung, liver, spleen, kidney, skeletal muscle (SKM), and brain. Real-time PCR revealed the biodistribution was highly localized to cardiac tissue. Off-target expression was primarily limited to the lung, liver, and spleen, with average expression levels of 2.1 ± 1.3, 0.78 ± 0.48, and 6.7 ± 2.2%, respectively, compared to expression in the heart (**Figure 4**). In the other organs, eGFPmodRNA expression was negligible, with values of 0.15 ± 0.11, 0.04 ± 0.02, and 0.04 ± 0.02% for kidney, SKM, and brain, respectively. The expression in all of these organs was significantly lower than in the heart ($P < 0.001$ versus heart), where dual-antibody staining revealed GFP expression in cells coexpressing the cardiac-specific marker α-actinin in striated sarcomeres (**Figure 4** inset, and **Supplementary Figure S3**).

In addition to the favorable biodistribution, there was no evidence of nanoparticle toxicity. Postsurgically, animals continued to thrive with a mean weight gain of 51.3 ± 18.5 gm in the 2 weeks following injection of 5 μg FLNP/modRNA, and they showed no overt signs of distress. Also, at the time of organ harvest, other than epicardial adhesions as expected after the previous thoracotomy procedure, there were no abnormalities found on macroscopic examination of the harvested organs.

Cardiac transduction achieved via intracoronary delivery of FLNP/modRNA

Having demonstrated myocardial transduction after direct injection of FLNP/modRNA nanoparticles into the ventricular wall, we explored an alternative method of administration that emulates the minimally invasive clinical approach of catheter-based intracoronary delivery. Using the aortic cross-clamping approach,[16] we found that adult rat myocardium was successfully transduced *in vivo* by FLNP via intracoronary delivery. At 20 hours after injection of FLNP/eGFPmodRNA at a dose of 10 μg as a single 500-μl bolus, eGFPmodRNA was clearly expressed in the heart (0.165 ± 0.097, $n = 4$), albeit at lower levels than by direct myocardial injection. Fluorescence microscopy revealed GFP-positive cells in the subepicardium of all treated hearts (**Figure 5** inset).

Biodistribution was evaluated as described above. As expected for intracoronary delivery to healthy myocardium, off-target expression was more pronounced than for direct intramyocardial injection, particularly in the lung, liver, and spleen (**Figure 5**), with average expression levels of 30.7 ± 8, 32.9 ± 4.5, and 80.5 ± 29.4%, respectively, compared to expression in the heart ($P = 0.051$, 0.063, and 0.969, respectively). Off-target expression levels in kidney, SKM, and brain were less than 5% of that in the heart ($P = 0.003$, 0.002, and 0.002, respectively). It is noteworthy that the actual level of eGFP mRNA in the spleen was comparable for intracoronary delivery (0.133 ± 0.049) and for direct myocardial delivery (0.231 ± 0.075, $P = 0.088$; unpaired t-test). Thus, the apparently high off-target splenic percentage in the former mainly reflects low retention in the heart rather than elevated retention in the spleen. These findings in healthy rat heart most likely underestimate the cardiac expression that would occur with intracoronary delivery to infarcted myocardium, in which diminished coronary flow and compromised endothelial integrity tend to enhance local retention of circulating nanoparticles.[17]

Consistent with the findings from direct intramyocardial injection, there was a pronounced decrease in eGFP mRNA expression in the heart 2 weeks after intracoronary delivery of FLNP/modRNA ($n = 2$), retaining less than 5% of the expression present at 20 hours postdelivery. While there was also a decrease in eGFP mRNA expression in off-target organs (**Figure 5**), the one that retained the most expression was the spleen (0.072 ± 0.045).

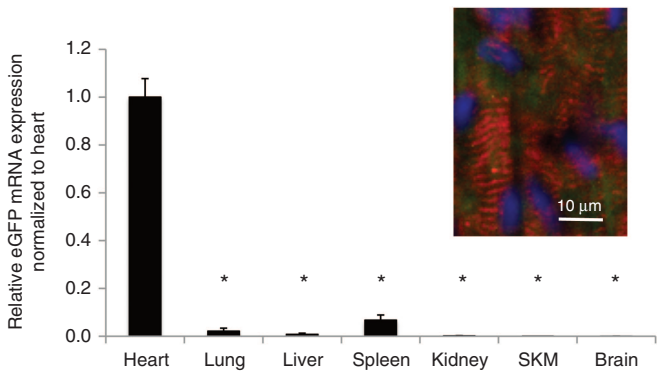

Figure 4 Biodistribution of eGFP mRNA after intramyocardial injection of FLNP/eGFPmodRNA in rats. Expression of eGFP mRNA measured by real-time PCR in organs harvested 20 hours after intramyocardial injection of formulated lipidoid nanoparticles (FLNP) with 5 μg of eGFPmodRNA. Values represent mean (±SD, $n = 3$ rats) eGFP mRNA expression levels relative to GAPDH, and normalized by mean expression in the heart. SKM, skeletal muscle. *$P < 0.001$ versus heart. Inset: Immunofluorescence of frozen tissue section of rat myocardium at 20 hours postinjection shows α-actinin-positive cells with sarcomeres (red) expressing GFP (green). Nuclei stained with DAPI (blue). Scale bar = 10 μm. DAPI, 4',6-diamidino-2-phenylindole.

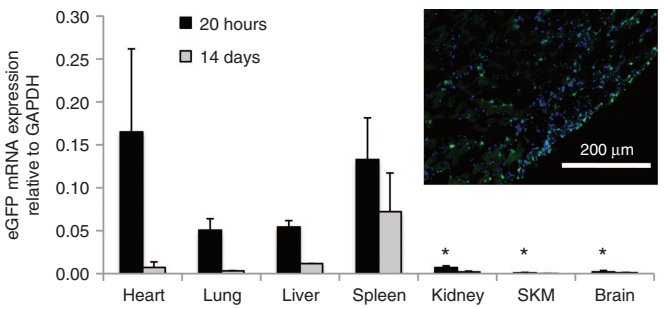

Figure 5 Intracoronary delivery of FLNP/eGFPmodRNA via left ventricle injection with temporary aortic cross-clamping in the rat. Bar graph displays the biodistribution of eGFP mRNA in organs harvested 20 hours (black bars, $n = 4$) and 14 days (gray bars, $n = 2$) after intracoronary delivery of formulated lipidoid nanoparticles (FLNP) with 10 μg of eGFP-modRNA. Values represent mean (±SD) expression levels of eGFP mRNA measured by real-time PCR relative to GAPDH. SKM, skeletal muscle. *$P < 0.005$ relative to heart at 20 hours; no statistical analysis was done for the 14-week samples. Inset: GFP expression in rat myocardium collected at 20 hours postdelivery, demonstrated by immunofluorescence of frozen tissue section incubated with anti-GFP antibody (green), and DAPI (blue). Scale bar = 200 μm. DAPI, 4',6-diamidino-2-phenylindole.

Pilot large animal study

Feasibility of FLNP/eGFPmodRNA nanoparticle delivery to the heart was also explored in healthy Yorkshire pigs, using open-chest intramyocardial injection and minimally invasive percutaneous intracoronary catheter-based delivery. To further explore the efficacy of FLNP/modRNA in the setting of cardiac disease, the same delivery approaches were also tested in postmyocardial infarction (MI) pigs ($n = 1$ pig for each pilot study condition).

For direct intramyocardial delivery, a 72-µg dose of FLNP/eGFPmodRNA solution was injected into the open-chest left ventricle (LV) free wall; after recovery for 20 hours the animal was euthanized and tissue samples were collected, providing cardiac expression data at 20 hours postinjection. GFP mRNA expression was detected in the areas of direct intramyocardial injections, with a level of expression (relative to GAPDH) of 13.03 ± 4.68 (**Figure 6a**). A sample of the LV remote from the areas of injection showed minimal GFP mRNA expression (0.33 ± 0.01), and virtually nothing was detected in an untreated sham animal (0.0084 ± 0.00003). Similar to observations in the rat, the GFP mRNA expression in off-target organs was lower than in the heart; with the highest off-target expression in the lung (3.91 ± 0.055), followed by the spleen (0.81 ± 0.049) and the liver (0.44 ± 0.0027). Immunofluorescence revealed GFP-positive cells through the full wall thickness in the injected heart samples, with no GFP detected in negative controls including remote LV myocardium (**Supplementary Figure S4**); dual immunostaining revealed the presence of GFP expression in cells positive for α-actinin (**Figure 6c**, and **Supplementary Figure S5**), indicating successful delivery to cardiomyocytes. GFP expression was also revealed in cardiac cells that stained positive for the putative fibroblast marker, vimentin (**Figure 6d**). In the spleen, GFP signal was observed in macrophages (MΦ) that stained positive for anti-MΦ antibody, as well as in elongated MΦ-negative cells (**Figure 6e**).

As an exploratory intervention to examine very early expression following FLNP/modRNA delivery in both injured and noninjured myocardium, open-chest intramyocardial injection was performed 20 minutes prior to sacrifice of a pig with chronic MI. FLNP/eGFPmodRNA injected into the infarct border zone (BZ) and into a nonischemic remote LV zone resulted in localized eGFP mRNA expression that was similar in both regions (6.53 ± 0.8 and 6.26 ± 0.06 respectively), with only minimal levels at a noninjected LV remote site (0.012 ± 0.0) (**Figure 6b**). Immunofluorescence revealed GFP expression in corresponding frozen tissue samples, just 20 minutes after the injection (**Figure 6b** inset and **Supplementary Figure S6**).

As a more clinically suitable minimally invasive delivery approach, a solution containing FLNP/eGFPmodRNA (500-µg dose in 10 ml PBS) was infused into the left main coronary artery of the pig via percutaneous femoral artery approach. As observed in the rat, coronary injection resulted in lower mRNA transfer compared to direct intramyocardial delivery at a matched time point of 20 hours postinjection. GFP mRNA was detected throughout the pig heart, with the highest levels in the posterior wall of the LV (0.077 ± 0.005) (**Figure 7a**). Off-target expression was higher than in the heart, with the highest expression in the spleen, lung, and liver (1.49 ± 0.116, 1.18 ± 0.075, and 0.51 ± 0.0104, respectively). Immunofluorescence of tissue sections from the heart revealed GFP expression in all regions (**Figure 7a**, left inset and **Supplementary Figure S7**).

Next, we examined if intracoronary delivery of FLNP/eGFPmodRNA in the acute MI setting would be similarly effective. To reflect the possible clinical application, nanoparticle injection was conducted 2 days after the ischemic reperfusion of the left anterior descending coronary artery. Consistent with findings in the healthy pig, eGFP mRNA was detected throughout the heart, with the highest level of expression in the

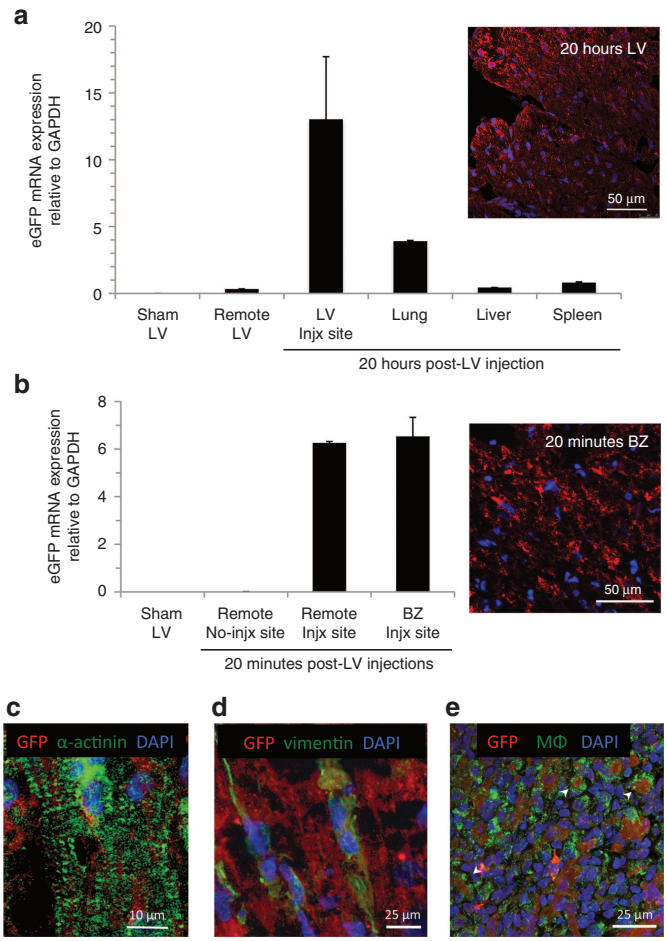

Figure 6 Direct intramyocardial delivery of FLNP/eGFPmodRNA in a pilot large animal study in healthy and diseased pigs. (**a**) Expression of eGFP mRNA in healthy pig myocardium 20 hours after intramyocardial injection of formulated lipidoid nanoparticles (FLNP) with 72-µg dose of eGFPmodRNA, compared to untreated sham animal. Biodistribution showed lower GFP expression in off-target organs than in the heart. Values represent mean (±SD) eGFP mRNA expression levels relative to GAPDH. (**b**) Expression of eGFP mRNA 20 minutes after intramyocardial injection of FLNP/eGFPmodRNA (36-µg dose) at two LV sites in a pig with heart failure at 12 weeks post-MI, compared to non-injection remote LV site and untreated sham animal. Insets: Immunofluorescence microscopy of frozen tissue sections of pig LV myocardium from subendocardium of injection site 20 hours postinjection in healthy pig (top inset) and from border zone (BZ) injection site at 20 minutes postinjection in MI pig (bottom inset) show expression of GFP (red). Nuclei stained with DAPI (blue). Scale bars = 50 µm. (**c–e**) Colocalization studies show GFP expression (red) in α-actinin-positive cardiomyocytes with sarcomeres (**c**), in vimentin-positive cardiac fibroblasts (**d**), and in macrophages (MΦ) in the spleen (**e**, arrows). Nuclei stained with DAPI (blue). Scale bars = 10, 25, and 25 µm as indicated. DAPI, 4',6-diamidino-2-phenylindole.

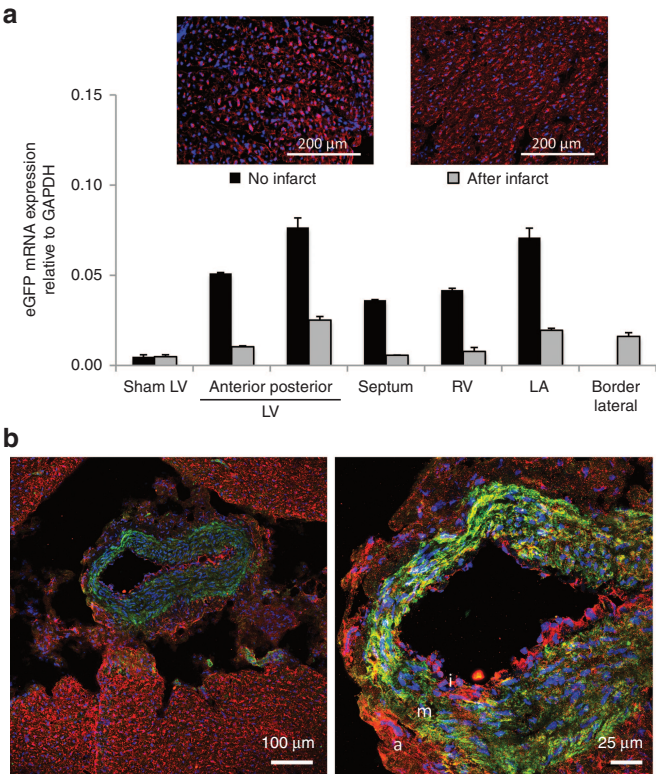

Figure 7 Intracoronary delivery of FLNP/eGFPmodRNA in a pilot large animal study in healthy and diseased pigs. (**a**) Expression of eGFP mRNA in healthy and diseased (48 hours post-MI) pig myocardium 20 hours after intracoronary injection of FLNP with 500 µg dose of eGFPmodRNA, comparing expression levels in different regions of the heart. LA, left atrium; LV, left ventricle; RV, right ventricle. Insets: Immunofluorescence of posterior LV frozen tissue sections from healthy (left inset) and postinfarct (right inset) hearts show GFP expression (red), and nuclei stained with DAPI (blue). Scale bars = 200 µm. (**b**) Immunofluorescent microscopy studies show GFP expression (red) colocalizes with α-smooth muscle actin-positive smooth muscle cells in the media (m) and also with cells in the intima (i) and adventitia (a) layers of the coronary vessel wall, which is surrounded by GFP-positive myocardial tissue. Scale bars = 100 and 25 µm, as shown. DAPI, 4',6-diamidino-2-phenylindole.

posterior wall of the LV (0.025 ± 0.0020). Infarct-related areas identified as anterior LV (0.010 ± 0.00055) and border lateral LV (0.016 ± 0.0021) had similar mRNA levels as the remote regions of the heart (**Figure 7a**). Although the mRNA distribution pattern appeared similar in the healthy and post-MI pigs, levels were consistently lower in the diseased animal, even in off target organs such as the spleen, where the GFP mRNA value (0.41 ± 0.09) was less than one-third of that observed in the healthy pig. GFP delivery was corroborated by immunofluorescence (**Figure 7a**, right inset), which revealed strong expression throughout the LV. Dual labeling of LV tissue revealed GFP expression in cells positive for α-smooth muscle actin; this was particularly evident in coronary vessels, where GFP expression was present in all three layers of the vessel wall, including the α-smooth muscle actin-positive smooth muscle cells in the tunica media, as well as cells within the outer tunica adventitia, and cells in the intima layer (**Figure 7b**). Cells in the surrounding myocardium were also GFP-positive.

DISCUSSION

The incidence of heart failure continues to increase worldwide despite advances in pharmacological therapy and assist devices. Therefore, the success of recent preclinical and clinical cardiac gene therapy trials has generated justifiable enthusiasm.[18,19] Nevertheless, as mentioned in the Introduction, limitations of traditional viral delivery of DNA motivate the active development of alternative vectors that allow controlled levels and duration of gene expression in the heart. The findings of this study demonstrate that our lipidoid-based FLNP nanoparticle formulation offers an effective nonviral agent for efficient cardiac delivery of modRNA in small and large animals, via multiple routes of administration, in healthy and disease hearts, using mRNA doses that are orders of magnitude lower than previous studies.[14]

Various interventional approaches have been reported to achieve gene transfer to the heart, ranging from highly invasive direct myocardial injection, to minimally invasive catheter-based procedures which are preferred for clinical applications.[1,16,20] The present study demonstrates effective cardiac delivery by direct intramyocardial injection in both rat and pig experiments, by intracoronary delivery in the rat using the invasive aortic cross-clamping procedure, and by minimally-invasive percutaneous catheter-based intracoronary delivery in the pig. In the rat model, intramyocardial injection resulted in GFP protein expression that was concentrated near the subepicardial injection sites, with little evidence of GFP signal in neighboring midwall and subendocardium. This result is consistent with the findings reported by Zangi *et al.*[14], of localized luciferase protein expression following intramyocardial injection of modRNA in the mouse. By contrast, in the porcine model, subepicardial injection resulted in robust GFP protein expression from epicardium to endocardium, despite a much thicker ventricular wall. It is unclear whether this difference reflects variation in transmural transport of FLNP nanoparticles, of dissociated modRNA, or of the translated protein, but such species-specific differences may have important implications for translating such technology to humans.

In both rodents and pigs, higher cardiac expression and lower off-target biodistribution were achieved by direct intramyocardial injection compared to the intracoronary approaches. This result was not unexpected considering the nontargeting FLNP formulation and healthy animal models used in this feasibility study. Using immunofluorescence and confocal microscopy, all of the cardiac cell types examined (myocytes, fibroblasts, smooth muscle cells, and endothelial cells) exhibited GFP expression, indicating no evidence of cell specificity for the nanoparticle formulation used in this study. Macrophages in the spleen were also GFP-positive. In the postinfarction conditions tested (direct injection in the setting of chronic MI, and intracoronary delivery in acute MI), the patterns of GFP mRNA expression were similar to observations in healthy animals, with no obvious differences in delivery when comparing injured versus remote regions of the same heart. Locally enhanced permeability and retention effects in the ischemic region of the heart[21,22] were expected to improve localized expression and cardiac retention with intracoronary delivery post-MI; however, this was not supported by our findings. If necessary, improved homing to infarcted myocardium may be engineered into the system by designing lipid-based nanoparticles

with surface molecules that promote tissue-specific or injury-specific targeting.[23]

The expression kinetics of mRNA are known to be fast-acting because translation occurs in the cytosol without having to cross the nuclear membrane, which is also advantageous for delivery to nondividing cells such as cardiomyocytes. Intracellular ribonuclease enzymes then cause degradation of mRNA within hours to days, leading to a transient expression profile. In the current study, rapid expression kinetics were confirmed by quantitative RT-PCR at time points ranging from 6 hours to 14 days postdelivery, showing a half-life of about 48 hours in the rat heart. The corresponding immunofluorescence microscopy analysis confirmed GFP protein expression at 6 hours, with peak expression observed at the 20-hour time point and negligible GFP signal by 60 hours in the heart, although GFP mRNA remained detectable by PCR in the spleen even at the 14-day time point. In the pig model, robust GFP protein expression was also observed at the 20-hour time point following intramyocardial and intracoronary delivery, and even in regions where FLNP/eGFPmodRNA was injected directly into the myocardium just 20 minutes prior to sacrifice. In prior *in vivo* mouse studies, the earliest time point reported was 2 hours after intramyocardial injection of GFPmodRNA with a polyethylenimine-based nanoparticle,[15] and at 4 hours after delivery of luciferase mRNA nanoparticles by intranasal, intravenous, and subcutaneous delivery methods; for the latter, in three out of four cases, maximum *in vivo* bioluminescence was observed at the 4-hour time point,[10] implying that the onset of protein synthesis must have occurred even earlier. For *in vitro* cell transfection studies, delivery of mRNA has resulted in significant protein expression as quickly as 1 hour post-treatment, with peak expression around 5–7 hours,[10,24] but no expression data were reported earlier than the 1-hour time point. Thus, our findings of GFP fluorescent signal at 20 minutes after injection of FLNP/eGFPmodRNA in the pig heart represent the most rapid protein expression following mRNA delivery that we are aware of to date.

The FLNP nanoparticle formulation also conferred efficiency in terms of the dosage of mRNA required for robust cardiac expression. For comparison, recent studies have shown mixed benefits of lipid-based nanoparticle-encapsulated mRNA (using Stemfect RNA Transfection Reagent) versus naked mRNA depending on the site of delivery.[10] We found that for direct intramyocardial injection in the rat, FLNP/modRNA unequivocally outperformed naked mRNA, resulting in over 60-fold higher mRNA levels and correspondingly higher protein expression at 20 hours postdelivery. The FLNP nanoparticle system was also superior to Stemfect for direct intramyocardial delivery of eGFP-modRNA, with RT-PCR revealing fourfold higher mRNA levels at 20 hours postdelivery in one pilot rat experiment using the 10-μg modRNA dose (not shown); an added practical benefit of FLNP/mRNA is the extended chemical stability at 4 °C storage, whereas StemfectRNA nanoparticles (an electrostatic complex using a proprietary lipid-like molecule) must be used within minutes of synthesis. Lipofectamine has also been used to deliver luciferase modRNA nanoparticles to mouse hearts by direct injection, requiring a dosage of 100 μg modRNA per mouse, or about 3.3 μg/g assuming a typical mouse body weight of 30 g. By comparison, FLNP nanoparticles required only 10 μg of modRNA for a 285-g rat, yielding a dose of 0.035 μg/g that is 100× more efficient than using Lipofectamine; efficiency was even better in the pig, where 72 μg modRNA yielded effective transduction in a 20 kg animal (0.0036 μg/g dose). Thus, to our knowledge, FLNP/mRNA nanoparticles offer the most efficient nonviral method of gene delivery to myocardium, requiring the lowest dosage of nucleotide per animal, which is advantageous to reduce expenses related to the high cost of synthesizing modified RNA, and to minimize potential adverse effects of off-target delivery.

Rats that survived FLNP delivery showed no overt side effects and continued to thrive for up to 2 weeks of monitoring. Cases of acute mortality were attributed to the challenging surgical interventions, particularly the aortic cross-clamping procedure. However, with intracoronary delivery in the healthy pig model, coronary spasm was detected in a portion of the coronary branches after the injection, which was partially reversed by nitroglycerin. However a small region of necrotic tissue was identified at the injection area during postmortem inspection, reflecting a possible combination of cardiotoxicity and vessel stimulatory effect using this delivery approach. Therefore, it would be premature to conclude that FLNP are completely safe, and careful investigation of local and off-target effects as well as short- and long-term safety are still required.

Limitations of this study include testing with a reporter gene only. Our team has recently demonstrated that adenoviral delivery of stem cell factor gene therapy leads to improved cardiac performance in small and large animal models of MI.[4,5] In fact, FLNP/SCFmodRNA treatment for MI represents a particularly interesting future application of our nanoparticle technology, capitalizing on the rapid onset but short duration of protein expression that could be ideal for transiently elevating homing of stem cells to the heart after infarction, without persistent stimulation of long-term uncontrolled growth.

Additional work is also needed to understand the biological mechanisms governing FLNP-mediated mRNA delivery to cardiac cells. This could include *in vitro* cell culture studies combined with 3D nanoparticle tracking technology.[25] However, preliminary *in vitro* testing using primary neonatal rat cardiomyocyte cultures showed poor transfection with FLNP/eGFPmodRNA that was not representative of the *in vivo* performance. Thus, development of more predictive in vitro screening models, possibly including 3D engineered cardiac tissue cultures,[26,27] may be essential for future optimization of therapeutic nanoparticles with specific cardiac affinity.

Conclusion

In conclusion, we have completed proof-of-concept studies supporting our hypothesis that formulated lipidoid nanoparticles carrying synthetic modified mRNA can be used for *in vivo* message delivery to cardiac cells in small and large animals. The rapid and transient expression is detectable on a time window from less than an hour to several days, with limited off-target biodistribution especially with direct intramyocardial delivery. Our formulation is also more efficient than prior nonviral carriers for cardiac gene therapy applications, reducing the required dosages of mRNA by two to three orders of magnitude. These results point toward the utility of the novel FLNP/modRNA platform for treating

acute and chronic MI in clinically relevant animal models, and prompts investigations using therapeutic modRNA. Thus, future applications of our FLNP/modRNA nanoparticles could complement existing gene therapy strategies by enabling safer nonviral approaches using clinically translatable delivery strategies and practical amounts of mRNA, to achieve transient expression of cardiotherapeutic proteins that could advance the field of cardiac regenerative medicine.

MATERIALS AND METHODS

FLNP/eGFPmodRNA. FLNP were created from modified mRNA (modRNA) combined with an active epoxide-derived lipidoid reagent, termed C14-113, and stabilizing lipid excipients including distearoyl phosphatidylcholine, cholesterol, and a polyethylene glycol-lipid conjugate. These cationic lipid-based nanoparticles were originally developed by the Anderson and Langer laboratories for delivery of small interfering RNAs.[8] The FLNP are obtained by nanoprecipitation of lipidoid with modRNA at high concentration followed by dialysis against PBS for a minimum of 3 hours at 4 °C. The commercially obtained reporter gene, eGFPmodRNA (Stemgent), was transcribed *in vitro* and incorporates both pseudouridine and 5-methylcytidine modified nucleotides to minimize the cellular interferon response to single-stranded RNA. Briefly, stock solutions of C14-113 lipidoid (MW 541, as synthesized in ref. 7), distearoyl phosphatidylcholine (MW 790), cholesterol (MW 387), and mPEG2000-DMG (MW 2660) were made in absolute ethanol at concentrations of 10 mg⁄ml, respectively. Components were combined to yield molar fractions of 50:10:38.5:1.5 at a lipidoid concentration of 4 mg/ml. eGFPmodRNA was diluted in 10 mmol/l citrate buffer at pH 3.0 to a concentration of 0.133 mg⁄ml, and the lipid mixture was added to the modRNA solution in a 3:1 v/v ratio to achieve a 10:1 w/w ratio of lipidoid to modRNA. After allowing 10 minutes at room temperature for particle self-assembly to occur, formulations were dialyzed against sterile-filtered PBS at pH 7.4 in 3,500 molecular weight cutoff dialysis cassettes (Pierce) for at least 3 hours or as long as overnight (for convenience) at 4 °C, and then maintained chilled until use.

Stability of the FLNP/modRNA nanoparticles was tested for up to 15 days of storage at 4 °C compared to freshly synthesized particles on day 0 of synthesis. Measurements included particle size by dynamic light scattering, and *in vitro* transfection efficiency determined from mean fluorescence intensity in cultured HeLa cells measured at 24 hours after transfection with 40 ng eGFPmodRNA. Particle sizes were measured on suspensions diluted 100-fold in PBS using a ZetaPALS dynamic light scattering detector (Brookhaven Instruments, Holtsville, NY, 15-mW laser, incident beam 676 nm). Correlation functions were collected at a scattering angle of 90°, and particle sizes were obtained from the MAS option of BIC's particle sizing software (v. 2.30) using the viscosity and refractive index of water at 25 °C. Particle sizes are expressed as effective diameters (z-average diameters) calculated using the Stokes-Einstein relationship from the diffusion coefficient obtained by cumulant analysis.

For *in vitro* experiments, 1 day before transfection, 12,500 HeLa cells (100 µl) were seeded into each well of a 96-well polystyrene tissue culture plate. FLNP/modRNA complexes in PBS (30 µl) were then gently mixed with fresh medium (195 µl) prewarmed to 37 °C. Conditioned medium was removed using a 12-channel aspirating wand and replaced with the complexes diluted in medium (150 µl) representing a dose of 40 ng eGFPmodRNA per well. Following 24-hour incubation, cells were washed with PBS and detached with 0.25% trypsin-ethylenediaminetetraacetic acid (25 µl, Life Technologies, Invitrogen, Grand Island, NY). FACS running buffer (50 µl), consisting of 98% PBS and 2% fetal bovine serum, was added to each well, then the cells were transferred to a 96-well round-bottom plate. GFP expression was measured using FACS on a BD LSR II (Becton Dickinson, San Jose, CA). Gating and analysis were performed using FlowJo v8.8 software (TreeStar, Ashland, OR).

Animal use. Surgical procedures were performed using adult male Sprague-Dawley rats obtained from a commercial supplier (Taconic Farms, Germantown, NY) and maintained under husbandry care at Mount Sinai. Female Yorkshire pigs (20 kg) were purchased from Animal Biotech Industries, PA. All animals received humane care in compliance with the "Guide for the Care and Use of Laboratory Animals" prepared by the National Academy of Sciences and published by the National Institutes of Health.[28] Animal protocols were approved by the Institutional Animal Care and Use Committee at The Icahn School of Medicine at Mount Sinai, which is accredited by the American Association for Accreditation of Laboratory Animal Care.

Distribution of animals for the study. This study was designed to achieve two main objectives: (i) to establish the efficacy of FLNP/modRNA for *in vivo* cardiac delivery, and (ii) to determine the kinetics of modRNA expression in the treated hearts. Additionally we investigated the biodistribution of the modRNA, we explored two alternative methods of delivery, and we conducted the first pilot study in healthy and postinfarction large animal models.

To establish the efficacy of FLNP/modRNA for *in vivo* cardiac delivery (**Supplementary Figure S1a**), animals were distributed among three experimental groups to receive direct intramyocardial injections of FLNP carrying eGFPmodRNA (FLNP/eGFPmodRNA) at one of three different dosages of modRNA (1, 5, or 10 µg, $n = 3$ per group). As controls, animals were injected either with sterile PBS only or with naked eGFPmodRNA (10 µg) for which we used PBS solution as the carrier in substitution for the FLNP ($n = 3$ per group). To test efficacy and biodistribution, these animals were sacrificed 20 hours after the injection, and organs including the heart, lung, liver, spleen, kidney, SKM, and brain were immediately harvested. Each of the organ samples was divided in two, with one portion embedded in optimal cutting temperature compound for cryosection and staining, and the other frozen and stored at −80 °C for later processing for real-time PCR as described below.

To determine the modRNA expression kinetics (**Supplementary Figure S1b**), animals received direct intramyocardial injections of FLNP/eGFPmodRNA at a dose of 5 µg of modRNA, and organs were harvested at 6 hours, 20 hours, 48 hours, 60 hours, 96 hours, 1 week, and 2 weeks ($n = 1–5$ per group), as described above.

A second study was conducted using an alternative route of administration designed to examine the feasibility of a less invasive preclinical procedure. As described below, this involved aortic cross-clamping to achieve intracoronary delivery of FLNP/eGFPmodRNA. For this approach, four rats received FLNP/eGFPmodRNA at a dose of 10 µg modRNA, and the animals were sacrificed 20 hours after the injection for organ harvest. And two rats were sacrificed 2 weeks after injection. Results from this group were compared to saline control and direct intramyocardial injection groups.

Direct intramyocardial injection. Adult male Sprague-Dawley rats weighing 215–350 g (245 ± 25 g) were anesthetized with an intraperitoneal injection of ketamine/xylazine (60–80 and 5mg/kg respectively), intubated with a 16G or 18G soft catheter and connected to a mechanical ventilator (CWE, model SAR-830/AP, Ardmore, PA) providing room air, and placed on a heating pad. A left thoracotomy incision was performed to expose the heart. The pericardium was incised and two 6-0 silk sutures were loosely tied lengthwise on the anterior wall of the left ventricle (LV) to serve as a visual reference. The solution to be delivered (600 µl of FLNP/eGFPmodRNA, naked eGFPmodRNA, or sterile saline) was loaded into a 1 cc syringe, and direct intramyocardial injections were performed with a 25G needle, inserting only the tip of the needle (<3 mm) into the ventricular wall at a 45° angle. Multiple injections of approximately 50 µl each were distributed throughout the anterior lateral and inferior wall of the LV, five on either side of the reference sutures. The chest was closed in layers, and the animals were allowed to recover. For postoperative analgesia, Buprenorphine (0.1–0.5 mg/kg) was administered subcutaneously every

12 hours during the first 72 hours after surgery. Animals were sacrificed for organ harvest at time points ranging from 6 hours to 2 weeks postsurgery.

Intracoronary delivery with aortic cross clamping. Adult male Sprague-Dawley rats (195–284 g) (232 ± 37 g) were anesthetized and intubated as described above, ventilated with supplemental oxygen, and maintained at room temperature. The cross-clamping procedure is described in detail elsewhere.[16] Briefly, the heart was exposed through a midline thoracotomy; gentle traction was applied to the thymus and the ascending aorta was identified. After dissection of the pericardium, a purse string suture (6-0 silk) was applied at the apex of the heart and a 24G catheter was inserted through the center of the purse string into the left ventricular cavity; immediately upon obtaining blood return, a 1 cc syringe containing 500 µl of FLNP/eGFPmodRNA solution (10 µg modRNA dose) was connected to the catheter. The ascending aorta was clamped and the FLNP/eGFP-modRNA solution was injected into the LV while maintaining the cross clamping on the aorta, the chamber was flushed twice by withdrawing and returning blood with the syringe, and the clamp on the aorta was released after 30 seconds. The catheter was then withdrawn from the left ventricle and the purse string was tied to close the entry point into the heart. The chest was closed and the animals were allowed to recover as above. The animals were sacrificed for organ harvest at 20 hours ($n = 4$) and at 2 weeks ($n = 2$) after nanoparticle injection.

Pilot preclinical large animal study. Feasibility of FLNP/eGFPmodRNA nanoparticle delivery to the heart was also tested in a pilot study on Yorkshire pigs, using both open-chest and minimally invasive procedures with and without MI. Chronic MI was induced by implanting an embolic coil after balloon occlusion of the left circumflex artery, and the modRNA intramyocardial injection was performed 3 months after the MI to more closely reflect clinical patients with transmural scar. Acute MI was induced by occluding the left anterior descending for 90 minutes using a percutaneous coronary balloon as previously described[29]; this acute MI model was used to test intracoronary delivery of FLNP/eGFPmodRNA. For direct intramyocardial injection, the animals ($n = 2$) were anesthetized with inhaled isoflurane (3%) and the heart was exposed through a left anterolateral thoracotomy, FLNP/eGFPmodRNA solution was prepared as above and delivered to the left ventricle by multiple direct intramyocardial injections. In the healthy pig, 18 injections of 50–150 µl volume each were distributed over three sites, for a total dose of 72 µg eGFPmodRNA (the reported GFP mRNA level for the LV injection site in **Figure 6a** was obtained by averaging PCR results from the three sites). The chest was closed and the animals were allowed to recover. A fentanyl patch was applied to relieve procedure-related pain. Twenty hours later, the pig was euthanized and tissue samples were immediately collected from the injection sites, a remote noninjected LV site, and from lung, liver, spleen, and ovary. For the chronic MI pig, two LV sites were chosen for injection of FLNP/eGFPmodRNA solution, one at the border zone (BZ) of the infarct and one remote to the infarct, administering at each site a total of 36 µg eGFPmodRNA. After 20 minutes postinjection, the pig was euthanized and cardiac tissue samples were harvested from each of the injection sites and from a remote noninjection site. Left ventricle tissue from a healthy sham pig ($n = 1$) was used as a negative control.

For minimally invasive percutaneous intracoronary catheter-based delivery, both in the healthy and acute MI models, the pigs ($n = 2$) were anesthetized and vascular access was established by puncture of the left femoral artery using the Seldinger technique, a 5Fr Hockey stick catheter (Cordis, Miami, Fl) was advanced to the left coronary artery, and after a coronary angiogram, two 0.014-inch coronary guide wires (Abbott HI-TORQUE ADVANCE, Santa Clara, CA) were introduced into the left anterior descending and left circumflex coronary arteries to fix the position of the catheter at the left main trunk.[30] A solution containing FLNP/eGFPmodRNA (500 µg eGFPmodRNA) was diluted in PBS (10 ml total volume); this dose represents a 100-fold increase from the 5-µg dose used in rats, accounting for the approximate relative mass of the pig versus the rat. The solution was infused into the left main coronary artery at 1 ml/minute flow rate, followed immediately by a 10 ml flush of saline solution at the same flow rate. A completion angiogram was performed to confirm adequate coronary perfusion. The animals were allowed to recover and were euthanized 20 hours after the procedure. To evaluate the efficiency and distribution of myocardial delivery, distinct regions of the heart were harvested and analyzed separately; these included: anterior wall of the LV, posterior wall of the LV, interventricular septum, right ventricle (RV), and left atrium; and in the acute MI model, a border lateral region was also sampled.

Measurement of mRNA levels. Relative mRNA levels were determined using two-step quantitative real-time PCR. Total RNA was extracted from the harvested organ samples using the RNeasy Isolation kit with on-column DNase I treatment to eliminate contaminating genomic DNA according to the manufacturer's protocol (Qiagen, Valencia, CA). About 1 µg total RNA was reverse transcribed using the High Capacity cDNA Reverse Transcription kit (Applied Biosystems, Carlsbad, CA). Quantitative RT-PCR was performed using iTaq SYBR Green Mastermix with Rox (Bio-Rad, Hercules, CA) using the model 7500 Real-Time PCR System (Applied Biosystems). The PCR protocol consisted of one cycle at 95 °C (3 minutes) followed by 40 cycles of 95 °C (15 seconds) and 60 °C (1 minute), followed by a dissociation step. The primers used in qPCR were eGFP (fwd 5′-GAA CCGCATCGAGCTGAA-3′, rev 5′-TGCTTGTCGGCCATGATATAG-3′) and GAPDH (fwd 5′-ACAAGATGGTGAAGGTCGGTGTGA-3′ rev 5′-AGCTTCCCATTCTCAGCCTTGACT-3′) as endogenous control (primers acquired from Integrated DNA Technologies, Coralville, IA). Quantitation of gene expression was determined using the relative standard curve method.[31] All samples were run in triplicate, and the average value for each sample was used to quantify mRNA expression based on the ratio of eGFP to GAPDH levels.

Immunofluorescence. For immunofluorescence, heart samples were frozen and embedded in Tissue-Tek OCT Compound (Sakura, Torrance, CA). Cryosections (10 µm) were fixed with 4% paraformaldehyde for 10 minutes, and blocked with 10% heat inactivated goat serum (in PBS-triton 0.1%) for 30 minutes. Samples were then incubated overnight (4 °C) with anti-GFP-fluorescein isothiocyanate conjugated antibody (1:150 dilution; ab6662; Abcam, Cambridge, MA), followed by counterstain with 4',6-diamidino-2-phenylindole (DAPI) and mounted in ProLong Gold antifade reagent (Life technologies, Grand island, NY). For dual staining in rat myocardium, the samples were incubated overnight (4 °C) with anti-GFP-FITC and anti-α-actinin (sarcomeric) (1:400 dilution; A7811, Sigma-Aldrich, St Louis, MO) antibodies; followed by anti-GFP-fluorescein isothiocyanate and AF 594 rabbit anti-mouse (1:400 dilution; A11062, Life Technologies) for 2 hours at room temperature; nuclei were stained with DAPI. Fluorescent images were obtained using a digital epifluorescent microscope (EVOSfl, Life Technologies).

Pig heart samples were treated with the following primary antibodies: mouse monoclonal anti-GFP (1:100, 632375, Clontech) rabbit anti-α-actinin (1:50, SC15335, Santa Cruz) chicken anti-vimentin (1:100, ab24525, abcam), mouse anti-α-smooth muscle actin (1:100, A5228, Sigma) mouse anti-pig macrophages (1:50, MCA2317GA, AbD Serotec) and rabbit polyclonal anti-GFP (1:100, 632592, Clontech) (this polyclonal antibody was used for the dual staining with the mouse anti-α-smooth muscle actin and the mouse anti-pig macrophages antibodies, in all other instances, the mouse monoclonal anti-GFP listed above was used); and secondary antibodies: donkey anti-mouse AF 555 (1:300, A31570, Life Technologies), goat anti-rabbit AF 488 (1:300, A11034, Life Technologies), goat anti-chicken AF 488 (1:200, A-11039, Life Technologies), donkey anti-mouse AF 488 (1:200, A21202, Life Technologies), and donkey anti-rabbit AF 546 (1:200, A10040, Life Technologies); for isotype control, we used mouse mAB IgG1 (1:125, 5415, Cell signaling); nuclei were stained with DAPI. Fluorescent images were obtained using a laser scanning confocal microscope (Leica TCS SP5 DMI, Leica Microsystems, Buffalo Grove, IL), a digital epifluorescent

microscope (EVOSfl, Life Technologies), and a Zeiss Axioplan2IE with ApoTome structured illumination technology.

Statistical analysis. Descriptive statistics are reported as mean and standard deviation. Differences between groups were evaluated based on univariate analysis of variance, with Scheffe's *post-hoc* test for multiple pairwise comparisons, using SPSS statistics software (IBM, Somers, NY). A P value <0.05 was considered statistically significant.

SUPPLEMENTARY MATERIAL

Figure S1. Schematic of research design for rat studies.
Figure S2. GAPDH mRNA levels normalized by input RNA after intramyocardial injection of FLNP/eGFPmodRNA in rats.
Figure S3. Dual immunofluorescence of rat myocardium after FLNP/eGFPmodRNA injection.
Figure S4. Representative images of GFP expression in pig heart tissue sections 20 hours after direct intramyocardial injection of FLNP/eGFPmodRNA.
Figure S5. Dual immunofluorescence of pig myocardium with and without FLNP/eGFPmodRNA injection.
Figure S6. Representative images of GFP expression in post-MI pig heart tissue sections 20 minutes after direct intramyocardial injection of FLNP/eGFPmodRNA.
Figure S7. Immunofluorescence of different regions of the pig heart following intracoronary injection of FLNP/eGFPmodRNA.

ACKNOWLEDGMENTS

The authors gratefully acknowledge Amy R. Kontorovich for assistance with lipid nanoparticle use *in vitro*, Lior Zangi for assistance with handling eGFPmodRNA, and Lauren Leonardson for providing excellent technical assistance and expertise with large animal studies. This work was funded by NIH/NHLBI Program of Excellence in Nanotechnology (PEN) Award, Contract No. HHSN268201000045C, and NIH/NHLBI T32HL007824, and by NIH R01 HL117505, HL119046, and a Transatlantic Fondation Leducq grant (R.J.H). Confocal microscopy was performed at the Microscopy CORE at the Icahn School of Medicine at Mount Sinai. D.G.A. serves as a consultant and has a grant on mRNA delivery from Shire, Plc. None of the other authors declare any potential conflicts of interest.

REFERENCES

1. Kawase, Y, Ly, HQ, Prunier, F, Lebeche, D, Shi, Y, Jin, H *et al.* (2008). Reversal of cardiac dysfunction after long-term expression of SERCA2a by gene transfer in a pre-clinical model of heart failure. *J Am Coll Cardiol* **51**: 1112–1119.
2. Zsebo, K, Yaroshinsky, A, Rudy, JJ, Wagner, K, Greenberg, B, Jessup, M *et al.* (2014). Long-term effects of AAV1/SERCA2a gene transfer in patients with severe heart failure: analysis of recurrent cardiovascular events and mortality. *Circ Res* **114**: 101–108.
3. Hayward, C, Banner, NR, Morley-Smith, A, Lyon, AR and Harding, SE (2015). The Current and Future Landscape of SERCA Gene Therapy for Heart Failure: A Clinical Perspective. *Hum Gene Ther* **26**: 293–304.
4. Yaniz-Galende, E, Chen, J, Chemaly, E, Liang, L, Hulot, JS, McCollum, L *et al.* (2012). Stem cell factor gene transfer promotes cardiac repair after myocardial infarction via in situ recruitment and expansion of c-kit+ cells. *Circ Res* **111**: 1434–1445.
5. Ishikawa, K, Fish, K, Aguero, J, Yaniz-Galende, E, Jeong, D, Kho, C *et al.* (2015). Stem cell factor gene transfer improves cardiac function after myocardial infarction in swine. *Circ Heart Fail* **8**: 167–174.
6. Thomas, CE, Ehrhardt, A and Kay, MA (2003). Progress and problems with the use of viral vectors for gene therapy. *Nat Rev Genet* **4**: 346–358.
7. Petros, RA and DeSimone, JM (2010). Strategies in the design of nanoparticles for therapeutic applications. *Nat Rev Drug Discov* **9**: 615–627.
8. Love, KT, Mahon, KP, Levins, CG, Whitehead, KA, Querbes, W, Dorkin, JR *et al.* (2010). Lipid-like materials for low-dose, *in vivo* gene silencing. *Proc Natl Acad Sci USA* **107**: 1864–1869.
9. Green JJ, ZG, Tedford NC, Huang YH, Griffith LG, Lauffenburger DA, Sawicki JA, Langer R, Anderson DG. (2007). Combinatorial modification of degradable poymers enables transfection of human cells comparablee to adenovirus. *Advanced Materials* **19**: 2836–2842.
10. Phua, KK, Leong, KW and Nair, SK (2013). Transfection efficiency and transgene expression kinetics of mRNA delivered in naked and nanoparticle format. *J Control Release* **166**: 227–233.
11. Andries, O, De Filette, M, De Smedt, SC, Demeester, J, Van Poucke, M, Peelman, L *et al.* (2013). Innate immune response and programmed cell death following carrier-mediated delivery of unmodified mRNA to respiratory cells. *J Control Release* **167**: 157–166.
12. Anderson, BR, Muramatsu, H, Nallagatla, SR, Bevilacqua, PC, Sansing, LH, Weissman, D *et al.* (2010). Incorporation of pseudouridine into mRNA enhances translation by diminishing PKR activation. *Nucleic Acids Res* **38**: 5884–5892.
13. Djurovic, S, Iversen, N, Jeansson, S, Hoover, F and Christensen, G (2004). Comparison of nonviral transfection and adeno-associated viral transduction on cardiomyocytes. *Mol Biotechnol* **28**: 21–32.
14. Zangi, L, Lui, KO, von Gise, A, Ma, Q, Ebina, W, Ptaszek, LM *et al.* (2013). Modified mRNA directs the fate of heart progenitor cells and induces vascular regeneration after myocardial infarction. *Nat Biotechnol* **31**: 898–907.
15. Huang, CL, Leblond, AL, Turner, EC, Kumar, AH, Martin, K, Whelan, D *et al.* (2015). Synthetic chemically modified mrna-based delivery of cytoprotective factor promotes early cardiomyocyte survival post-acute myocardial infarction. *Mol Pharm* **12**: 991–996.
16. del Monte, F and Hajjar, RJ (2003). Efficient viral gene transfer to rodent hearts in vivo. *Methods Mol Biol* **219**: 179–193.
17. Paulis, LE, Geelen, T, Kuhlmann, MT, Coolen, BF, Schäfers, M, Nicolay, K *et al.* (2012). Distribution of lipid-based nanoparticles to infarcted myocardium with potential application for MRI-monitored drug delivery. *J Control Release* **162**: 276–285.
18. Dunlay, SM and Roger, VL (2014). Understanding the epidemic of heart failure: past, present, and future. *Curr Heart Fail Rep* **11**: 404–415.
19. Storrow, AB, Jenkins, CA, Self, WH, Alexander, PT, Barrett, TW, Han, JH *et al.* (2014). The burden of acute heart failure on U.S. emergency departments. *JACC Heart Fail* **2**: 269–277.
20. Hayase, M, Del Monte, F, Kawase, Y, Macneill, BD, McGregor, J, Yoneyama, R *et al.* (2005). Catheter-based antegrade intracoronary viral gene delivery with coronary venous blockade. *Am J Physiol Heart Circ Physiol* **288**: H2995–H3000.
21. Scott, RC, Crabbe, D, Krynska, B, Ansari, R and Kiani, MF (2008). Aiming for the heart: targeted delivery of drugs to diseased cardiac tissue. *Expert Opin Drug Deliv* **5**: 459–470.
22. Yao, C, Shi, X, Lin, X, Shen, L, Xu, D and Feng, Y (2015). Increased cardiac distribution of mono-PEGylated Radix Ophiopogonis polysaccharide in both myocardial infarction and ischemia/reperfusion rats. *Int J Nanomedicine* **10**: 409–418.
23. Gianella, A, Mieszawska, AJ, Hoeben, FJ, Janssen, HM, Jarzyna, PA, Cormode, DP *et al.* (2013). Synthesis and *in vitro* evaluation of a multifunctional and surface-switchable nanoemulsion platform. *Chem Commun (Camb)* **49**: 9392–9394.
24. Zou, S, Scarfo, K, Nantz, MH and Hecker, JG (2010). Lipid-mediated delivery of RNA is more efficient than delivery of DNA in non-dividing cells. *Int J Pharm* **389**: 232–243.
25. Welsher, K and Yang, H (2014). Multi-resolution 3D visualization of the early stages of cellular uptake of peptide-coated nanoparticles. *Nat Nanotechnol* **9**: 198–203.
26. Turnbull, IC, Karakikes, I, Serrao, GW, Backeris, P, Lee, JJ, Xie, C *et al.* (2014). Advancing functional engineered cardiac tissues toward a preclinical model of human myocardium. *FASEB J* **28**: 644–654.
27. Turnbull, IC, Lieu, DK, Li, RA, and Costa, KD (2012). Cardiac tissue engineering using human stem cell-derived cardiomyocytes for disease modeling and drug discovery. *Drug Discov Today Dis Models* 9: e219–e227.
28. Committee to Revise the Guide for the Care and Use of Laboratory Animals; National Research Council. *Guide for the Care and Use of Laboratory Animals*. National Academy Press, Washington DC, 1996.
29. Ishikawa, K, Aguero, J, Tilemann, L, Ladage, D, Hammoudi, N, Kawase, Y *et al.* (2014). Characterizing preclinical models of ischemic heart failure: differences between LAD and LCx infarctions. *Am J Physiol Heart Circ Physiol* **307**: H1478–H1486.
30. Ishikawa, K, Fish, KM, Tilemann, L, Rapti, K, Aquero, J, Santos-Gallego, CG *et al.* (2014). Cardiac I-1c overexpression with reengineered AAV improves cardiac function in Swine ischemic heart failure. *Mol Ther* **22**: 2038–2045.
31. Dhanasekaran, S, Doherty, TM and Kenneth, J; TB Trials Study Group (2010). Comparison of different standards for real-time PCR-based absolute quantification. *J Immunol Methods* **354**: 34–39.